International Journal of Pharmaceutics 366 (2009) 31–37

Contents lists available at ScienceDirect

International Journal of Pharmaceutics

journal homepage: www.elsevier.com/locate/ijpharm

Network structure and macromolecular drug release from poly(vinyl alcohol) hydrogels fabricated via two crosslinking strategies

Damia Mawad, Ross Odell, Laura A. Poole-Warren*

Graduate School of Biomedical Engineering, The University of New South Wales, Sydney, NSW 2052, Australia

ARTICLE INFO

Article history:
Received 9 July 2008
Received in revised form 26 August 2008
Accepted 26 August 2008
Available online 3 September 2008

Keywords:
PVA hydrogels
Redox curing
Drug delivery
Networks

ABSTRACT

Injectable hydrogels have potential biomedical applications ranging from tissue fillers to drug delivery vehicles. This study focussed on evaluating the structure of poly(vinyl alcohol) (PVA) hydrogels of variable solid content and high molecular weight model drug release from the networks formed via either conventional photo-polymerization compared with chemical initiation of polymerization using an oxidation–reduction (redox) reaction. Swelling behaviour was characterised in water to assess the structural properties. Model drugs, FITC-Dextran, 20 kDa (FD20) and 4 kDa (FD4) were loaded in the hydrogels prior to curing and drug release studies conducted. Redox-cured hydrogels were more swollen than UV-cured systems, lost ~20% of their polymer mass compared to only 5% from UV-cured hydrogels and subsequently exhibited networks of larger mesh sizes. Also, networks of variable solid contents showed different structural properties with systems of higher polymer concentration exhibiting a smaller mesh size. The difference in structural properties of the networks affected release of FD20, being faster in redox-cured than UV-cured hydrogels, and slower from systems of higher solid content. Release of FD4 was faster than FD20 from networks of same solid content. This study suggested that PVA hydrogels can be cured by redox-initiation to function as a controlled delivery system for macromolecular drugs.

1. Introduction

Hydrogels are formed from hydrophilic polymer chains held together by chemical or physical crosslinks. They are characterised by their ability to uptake large amounts of water while retaining their three dimensional structure. A variety of physical and chemical methods have been used to fabricate biomedical hydrogels and it is clear that crosslinking method can impact significantly the micro- and nanostructure of the resulting hydrogel (Peppas, 1987; Anseth et al., 2002; Mawad et al., 2007).

Freeze-thaw methods have been proposed for hydrogels like poly(vinyl alcohol) (PVA) hydrogels due to the characteristic crystallinity produced in these materials following exposure to repeated freezing and thawing cycles (Peppas, 1987). Many researchers adopted this method to study diffusive characteristics of the hydrogel (Hassan et al., 2000; Mongia et al., 1996). This method involves putting the polymer solution through repeated freeze–thaw cycles that result in a pre-formed implant. As a result of the underlying mechanism of this approach, injectable delivery is not possible and surgery is required to implant the device at the target site.

Radiation crosslinking using gamma radiation (Berkowitch et al., 1957; Peppas and Merrill, 1977) or exposure to ultraviolet (UV) light (Anseth et al., 2002) are alternative efficient methods that do not require high concentrations of extraneous chemicals and therefore result in clean hydrogels with low levels of extractable. Photoinitiators added to generate radicals that catalyse UV and visible light photocrosslinking have been investigated extensively for their cytotoxicity and several photoinitiators have been proposed for biomedical use (Bryant et al., 2000).

All of these methods produce pre-formed hydrogels with a range of structures and properties. The demand for injectable hydrogels for applications ranging from macromolecular drug delivery (Langer, 1998; Li et al., 2003) to embolotherapy (Siskin et al., 2000; Patel et al., 2005) and even tissue engineering (Shu et al., 2004; Nguyen and West, 2002), has led to the need for more versatile methods for crosslinking polymers *in situ* such as chemical crosslinking. In the past, chemical processing agents such as glutaraldehyde (Burczak et al., 1994) and epichlorohydrin (Bo, 1992) have been used to form PVA hydrogels. These have the disadvantage of being cytotoxic and potentially carcinogenic, limiting widespread biomedical use. Also, if the biomaterial is designed to function as a drug delivery system, toxic

* Corresponding author. Tel.: +61 2 9385 3905; fax: +61 2 9663 2108.
E-mail addresses: damia@uow.edu.au (D. Mawad), r.odell@unsw.edu.au (R. Odell), L.Poolewarren@unsw.edu.au (L.A. Poole-Warren).

0378-5173/$ – see front matter © 2008 Elsevier B.V. All rights reserved.
doi:10.1016/j.ijpharm.2008.08.038

residues may lower the bioactivity of the drug (Scotchford et al., 1998).

Another approach is use of oxidation–reduction (redox) reaction coupling to generate free-radicals under mild conditions to initiate the crosslinking process. Many redox systems have been used for radical initiation of polymerization, including the redox pair of hydrogen peroxide and ferrous salt employed in this paper (Sarac, 1999). More recently, redox curing has been studied for application to injectable hydrogels and although toxicity of oxidative components can be a concern, the final hydrogels formed tend to have low cytotoxicity (Mawad et al., 2007; Martens et al., 2008). Redox-cured hydrogels can be prepared and injected as a two part liquid system, with the reductant being in one part and the oxidant in the other part. The two parts are typically mixed during delivery and the redox reaction generates radicals so that curing takes place over a period of time *in situ* following mixing. Another advantage of this system is the capacity to suspend macromolecular drugs in the liquid hydrogel which then polymerises *in situ* via redox initiation. However, while efficient generators of free-radicals, redox systems have the potential disadvantage of non-uniformity of curing, and hence the resulting network structure of redox-cured hydrogels may impact on the drug delivery from the *in situ* cured hydrogel.

This study aimed to examine swelling properties, hydrogel structure and release of macromolecular compounds from PVA hydrogel delivery systems fabricated via either UV light or redox initiation. The effect of polymer concentration in the network and the size of the drug on release rate were also evaluated. For this purpose, FITC-Dextran was chosen as a model drug because of its availability in a range of molecular weight (MWs).

2. Materials and methods

2.1. Materials

PVA (14 kDa, 83% hydrolysed; BioCure Inc., Atlanta, GA), functionalised with seven acrylamide groups per chain was used to produce hydrogels. The chemical structure of the macromer is shown in Fig. 1. Stock aqueous hydrogel solutions of 30 wt.% polymer containing 0.05 wt.% of the photo-initiator 2-hydroxy-1-[4-(2-hydroxyethoxy)phenyl]-2-methyl-1-propanone (Irgacure 2959, Ciba Specialty Chemicals) were diluted in deionized water (DI-H_2O) to final concentrations of 10, 15, and 20 wt.% PVA. Fluorescein *iso*-thiocyanate dextran (FD20: 20 kDa, Stokes' radius = 33 Å and FD4: 4 kDa, Stokes' radius = 14 Å), ferrous gluconate dihydrate, L-ascorbic acid, hydrogen peroxide, and Dulbecco's phosphate buffered saline were purchased from Sigma and used without any further purification.

2.2. Fabrication of PVA hydrogels

PVA hydrogels were fabricated from 10, 15 and 20 wt.% solutions. Hydrogels were crosslinked into cylindrical shapes using a 1 ml syringe barrel as a mould (length ~1 cm, radius ~0.24 cm) by photo-initiation or redox initiation at room temperature in the range of 20–25 °C. UV-cured hydrogels were formed by exposure to UV light for 2 min using a Green Spot UV system (UV Source, Torrance, CA) (peaks at 310 and 365 nm) at an intensity of $\sim 1.79 \pm 0.09\ W/cm^2$. Exposure time of 2 min was determined based on the minimum time required for curing the 10 wt.% solutions. Curing was confirmed by the absence of residual fluid after removing the hydrogel sample from the mould.

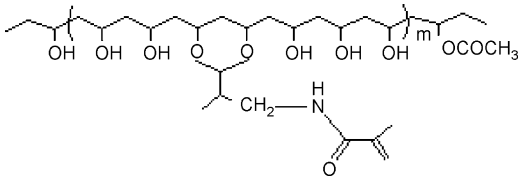

Fig. 1. Chemical structure of PVA (14 kDa, 83% hydrolysed) functionalised with seven acrylamide groups per chain as supplied by BioCure Inc., Atlanta, GA.

Redox initiation was achieved using ferrous gluconate as a reductant and hydrogen peroxide as an oxidant. The reaction generating the hydroxyl radicals is shown in Eq. (1) (Sarac, 1999):

$$Fe^{2+} + H_2O_2 \rightarrow HO^{\bullet} + Fe^{3+} + OH^{-} \quad (1)$$

Two solutions of same polymer concentration but with different composition, reductant or oxidant, were prepared. The final reductant solution contained 92.6 ppm of ferrous gluconate dihydrate and 292 ppm of ascorbic acid, and the oxidant solution contained 564 ppm of hydrogen peroxide. Two syringes containing equal volumes of each solution were connected via a dual connector. The plungers of the syringes were pushed back and forth to mix the two solutions until resistance was felt implying that the hydrogels were formed.

2.3. Equilibrium swelling studies

Wet weights of all PVA cylinders were measured at fabrication (m_i). To calculate the experimental initial polymer weight fraction (f_{pi}) in the fabricated networks, half of the samples were dried immediately after synthesis for 4 days at 85 °C and then reweighed (m_d). f_{pi} was then calculated as follows:

$$f_{pi} = \frac{m_d}{m_i} \quad (2)$$

The remaining samples were incubated in water at 37 °C. At different time points, samples were removed from water, blotted gently with filter paper and wet weight of swollen samples (m_{st}) was determined. The samples were then immersed in water and left to swell. This procedure was repeated until equilibrium was reached. Relative change in wet weight was calculated as follows:

$$\text{relative } \Delta(\text{wet weight}) = \frac{m_{st} - m_i}{m_i} \quad (3)$$

When the swollen samples reached a constant equilibrium weight (m_{se}), they were dried for 4 days at 85 °C and weighed (m_{pe}). The initial polymer mass (m_{pi}) in each sample was calculated by multiplying (m_i) by f_{pi}.

To assess polymer loss during equilibration, the polymer weight loss ratio (LR) was calculated as follows:

$$LR = \frac{m_{pe}}{m_{pi}} \quad (4)$$

Ratio less than 1 indicates that polymer has been lost from the network.

The structural properties of the networks were determined from the swelling studies. The volumetric swelling ratio (Q) of the hydrogels was determined after reaching equilibrium as follows (Peppas, 1987):

$$Q = 1 + \frac{\rho_{polymer}}{\rho_{solvent}}(q_e - 1) \quad (5)$$

where $\rho_{polymer} = 1.2619\ g/cm^3$, $\rho_{solvent}$ is the density of water ($1\ g/cm^3$) and q_e is the equilibrium mass swelling ratio calculated as

$$q_e = \frac{m_{se}}{m_{pe}} \quad (6)$$

The molecular weight between crosslinks ($\bar{M}_c$) was calculated based on the Peppas–Merill model as follows (Peppas et al., 2000):

$$\frac{1}{\bar{M}_c} = \frac{2}{\bar{M}_n} - \frac{(\bar{\upsilon}/v_1)[\ln(1-\upsilon_{2,s}) + \upsilon_{2,s} + \chi\upsilon_{2,s}^2]}{\upsilon_{2,r}\left[(\upsilon_{2,s}/\upsilon_{2,r})^{1/3} - (1/2)(\upsilon_{2,s}/\upsilon_{2,r})\right]} \quad (7)$$

where $\bar{M}_n$ is the number-average molecular weight of PVA before crosslinking (14,000 g/mol), $\bar{\upsilon}$ is the specific volume of the bulk polymer (0.788 cm^3/g), v_1 is the molar volume of water as the solvent (18 cm^3/mol), χ is the polymer–solvent interaction parameter (0.494), and $\upsilon_{2,r}$ and $\upsilon_{2,s}$ are the polymer volume fraction in the relaxed and swollen state respectively determined experimentally by weight analysis.

From the calculated $\bar{M}_c$, the mesh size (ζ) was calculated from:

$$\zeta = \upsilon_{2,s}^{-1/3}\left(\frac{2C_n\bar{M}_c}{M_r}\right)^{1/2} l \quad (8)$$

where C_n is the Flory characteristic ratio (8.8), l is the length of the C–C bond along the backbone chain (1.54 Å), and M_r is the molecular weight of PVA repeating unit (44 g/mol). The crosslinking density (ρ) was calculated from (Peppas, 1987):

$$\rho = \frac{1}{\bar{\upsilon}\bar{M}_C} \quad (9)$$

Two experiments were performed for each polymer concentration and each experiment included three specimens.

2.4. Release studies

Loaded-PVA hydrogels were fabricated from 10, 15 and 20 wt.% solutions containing 0.125 wt.% FD20. Briefly, a stock solution of FD20 in DI-H_2O (5 mg/ml) was prepared. 0.5 ml of the prepared stock solution was added to 1.5 ml of the polymer aqueous solution to produce 0.125 wt.% FD20 of the total volume. The solutions were then vortexed to ensure proper mixing. The macromer solutions were crosslinked using either UV or redox methods as described. The hydrogels were weighed at fabrication and the initial loading of the drug (M_{init}) was calculated based on the volume of the hydrogel. Loaded-PVA cylinders were incubated in 50 ml PBS (pH 7.4) at 37 °C on an orbital shaker. At different time points, 1 ml samples were taken and replaced by same volume of fresh PBS. All samples were stored frozen for 2 weeks and then analysed using a fluorescence micro-plate reader (f_{max}) at λ = 490–538 nm to determine the amount released (M_t). M_t was calculated from a standard curve of known concentrations of FITC-Dextran solutions in the range of 0–10 μg/ml. Standard curves were linear ($R^2 > 0.95$) within FD20 concentration range at least ten times higher than the concentration of FD20 in test samples. In addition, the analytical method was validated over time by measuring the same standard samples before and after freezing without observing any change in the corresponding fluorescence values.

The same procedure was followed for release of FD4 (4 kDa) from 10 and 15 wt.% UV-cured hydrogels. Three experiments were performed to assess the release of drug from each polymer concentration and each experiment included three replicates.

2.4.1. Theoretical model

A Fickian diffusion model (Crank, 1975), describing diffusion from an infinitely long cylinder as derived by Crank, was used to predict the release behaviour from the cylindrical PVA hydrogels. Diffusion of solutes from an infinitely long cylinder can be described as

$$\frac{\partial C}{\partial t} = -D\frac{\partial^2 C}{\partial r^2} \quad (10)$$

The initial and boundary conditions being:

$$C = f(r) \quad \text{if } 0 < r < a \text{ and } t = 0$$

$$C = 0 \quad \text{if } r = a \text{ and } t \geq 0$$

where r is the inner radius of the cylinder, a is the radius of the cylinder, C is the concentration of the solute dispersed in the cylinder, and t is the release time. For a volume of sink much bigger than the volume of the hydrogel and for small times, the analytical solution for Eq. (11) is

$$\frac{M_t}{M_{inf}} = \frac{4}{\pi^{1/2}}\left(\frac{Dt}{a^2}\right)^{1/2} - \frac{Dt}{a^2} - \frac{1}{3\pi^{1/2}}\left(\frac{Dt}{a^2}\right)^{3/2} + \cdots \quad (11)$$

where M_{inf} is the total amount of drug released into the sink, a is the radius of the cylinder, and D is the diffusion coefficient of the solute through the hydrogel.

To predict the theoretical diffusion coefficient (D_{Theor}) from non-degradable PVA hydrogels, Davis model (Davis, 1974) was used:

$$D_{Theor} = D_W \exp[-(5 + 10^{-4} \times MW_{Solute}) \times [Polymer]] \quad (12)$$

where MW_{Solute} is the molecular weight of the solute, [Polymer] is the concentration of the polymer in the hydrogel matrix, and D_W is the solute diffusion coefficient in water calculated according to Stokes–Einstein equation (Einstein, 1956).

2.4.2. Transformation of experimental data

As will be outlined in the result section, experimentally all hydrogels displayed an initial release at time zero. To be able to compare the experimental release to the theoretical model, the burst effect was eliminated by transformation of the experimental data. For each hydrogel, the amount of drug released (M_t) was plotted versus square root of time. A regression line was fitted to the linear part of the curve and the slope (s) and intercept (i) were calculated from the linear fit. The total amount released (M_{inf}) was estimated by fitting an asymptote to the plateau region of the curve and based on its value the % total release was calculated ($(M_{inf}/M_{init}) \times 100$).

To eliminate the burst effect from the experimental data, the amount released was transformed as follows:

$$\frac{M'_t}{M'_{inf}} = \frac{M_t - i}{M_{inf} - i} \quad (13)$$

To normalise the x-axis, all time points, t, were divided by t^* which was calculated from:

$$t^* = \left(\frac{M_{inf} - i}{s}\right)^2 \quad (14)$$

t^* is a characteristic time which might be taken as a release time.

For adjusted amount released of the drug, $M'_t/M'_{inf} < 0.6$, the experimental diffusion coefficient D was calculated from the slope of M'_t/M'_{inf} versus $t^{1/2}$ according to

$$\frac{M'_t}{M'_{inf}} = 4\sqrt{\frac{Dt}{\pi a^2}} \quad (15)$$

2.5. Statistical analysis

Results of the swelling experiments were analysed by two-way analysis of variance for the effects of polymer concentration and curing method. Analysis of variance was performed using Stata (StataCorp, 1999). The release study was performed as a series of experiments in which one cross linking method was used to produce gels at three concentrations. Three experiments were conducted with each crosslinking method. The results were analysed

as a split-plot design according to Armitage and Berry (1994). Comparison of crosslinking methods was based on comparisons between experiments and comparisons among polymer concentrations were based on comparisons within experiments. Analysis of variance was performed using Stata (StataCorp, 1999).

3. Results and discussion

3.1. Swelling studies

Swelling studies showed that varying the curing technique leads to the fabrication of networks of variable structural properties. Table 1 shows experimental initial polymer fraction (f_{pi}) in fabricated hydrogels at synthesis and polymer weight loss ratio (LR) after 4 days incubation for both UV- and redox-cured hydrogels. Experimental f_{pi} of UV-cured hydrogels were comparable to the theoretical values: 0.1, 0.15 and 0.2. However, the experimental values of f_{pi} of redox-cured hydrogels were higher for all concentrations. After mixing the reductant/oxidant solutions, allowing time for curing, and then pushing the hydrogel from the syringe, it was observed that some 'free' water was ejected along with the cured hydrogel. This might indicate that all the available water was not entrapped within the redox-cured hydrogel bulk due to in-efficiency in mixing, hence explaining the discrepancy in the measured f_{pi}. For the UV-cured hydrogels, where the measured f_{pi} matched expectations, no water was observed upon ejection from the syringe.

The inefficiency of mixing was further suggested by the lower LR of redox-cured hydrogels. There was significant difference between the crosslinking methods with redox-cured hydrogels losing approximately 20% polymer mass compared with the corresponding UV-cured hydrogels which lost up to 5% of polymer mass ($p < 0.0001$). On the other hand, polymer concentration had no significant effect on polymer loss from the network over time ($p = 0.7$). Efficient crosslinking by redox initiation depends on the efficiency of mixing the two solutions. The 20% mass loss suggests that crosslinking was not as efficient or complete in the redox gels. Inhomogeneous mixing may result in unequal distribution of the oxidant and reductant components. Regions with better mixing will have more efficient free radical generation resulting in the PVA chains in the vicinity to crosslink quickly (Mellot et al., 2001). However, in regions of lower concentration fewer free radicals are available and the probability for crosslinking of PVA chains is likely to be lower. These uncrosslinked chains remain free and unbound by kinetic chains to the network (Mellot et al., 2001; Anseth et al., 1994). Also, double bonds of same polymer chains might react together forming primary cycles that are not part of the network. As a result the hypothetical network structure can be described by a combination of microgel domains with complete conversion of double bonds and regions with light or no crosslinking. During incubation, these primary cycles and unbound chains are free to leach out of the network resulting in the polymer loss observed.

Table 1
% Initial polymer weight fraction (f_{pi}) and polymer weight loss ratio (LR) of UV- and redox-cured hydrogels

Crosslinking method	[Polymer] (%)	f_{pi}	LR
UV	10	0.10	0.99 (0.14)
	15	0.16	0.95 (0.06)
	20	0.22	0.94 (0.04)
Redox	10	0.13	0.80 (0.14)
	15	0.19	0.81 (0.04)
	20	0.26	0.80 (0.07)

Mean (standard deviations), $n = 6$.

However, the mass loss observed from redox initiation should not impose any limitation for the use of this technique because PVA as a low MW water-soluble polymer has a high rate of elimination from the body and minimal adverse biological reactions have been associated with PVA (Yamaoka et al., 1995).

Furthermore, UV- and redox-cured hydrogels exhibited differences in their water uptake and structural properties. Table 2 presents the experimental values of the volumetric swelling ratio (Q), the molecular weight between crosslinks ($\bar{M}_c$), the mesh size (ζ), and the crosslinking density (ρ). Q was greater for redox-cured hydrogels. Monitoring the wet weight of hydrogels during incubation time, it was observed that the wet weight of UV-cured hydrogels was dropping and the % relative change in wet weight was ~−10% as measured at equilibrium. Based on the measured LR that suggested only a 5% polymer loss from UV-cured hydrogels, it can be inferred that the drop in wet weight is also due to water loss. On the other hand, even though redox-cured hydrogels had a polymer mass loss of ~20%, the 10 and 15 wt.% hydrogels had a % relative change in wet weight in the order of 5%. Similarly, the wet weight of 20 wt.% redox-cured hydrogels increased by 10%. This increase in weight suggests an uptake of water by the redox-cured networks. Another factor that had an influence on the volumetric swelling ratio is the polymer concentration. Q decreased with polymer concentration suggesting that a more concentrated network looses less water in case of UV and swells more in case of redox-cured hydrogels.

The theoretical $\bar{M}_c$ for the PVA used in this study (seven crosslinkers per chain) is 2000 g/mol. The calculated value of $\bar{M}_c$ (1914 g/mol) of the 10 wt.% UV-cured hydrogels was comparable to this. However, as polymer concentration increased, $\bar{M}_c$ decreased from 1914 to 762 g/mol for UV cured and from 2801 to 1420 g/mol for redox-cured hydrogels as shown in Table 2. The decrease in $\bar{M}_c$ might be due to chain interactions and entanglements present in more concentrated polymer solutions. Redox-cured hydrogels had higher values of $\bar{M}_c$ at all concentrations which can be related to the inefficiency of the crosslinking method that caused a higher polymer mass loss and therefore caused polymer chains to be more physically distant in the network. Values of the mesh size decreased as the polymer concentration increased. Similar correlation between ζ and the polymer concentration has been reported in the literature (Hickey and Peppas, 1995; Cruise et al., 1998). Equilibrium swelling studies showed that redox-cured hydrogels swell more than UV-cured systems; subsequently the structural properties of the two systems were varied.

3.2. Release studies

Release studies were conducted to compare the effect of polymer concentration and crosslinking methods on the release of macromolecules from PVA hydrogels. All hydrogels exhibited an initial release at time zero presumably due to the instantaneous release of drug on the surface of the hydrogel. Values of burst % are listed in Table 3. No significant difference was observed between burst effects measured from networks of different polymer concentration or crosslinking methods ($p = 0.06$ and 0.9, respectively).

To be able to compare the experimental release to the theoretical model, the burst effect had to be eliminated and the experimental data was transformed as discussed in the method section. Fig. 2 is an illustrative example of the transformed experimental data for 10% UV- and redox-cured hydrogels. Three parameters were inferred including % total release, a characteristic or release time, and experimental diffusion coefficient. Their values are listed in Table 3.

Values of diffusion coefficients decreased with increase in polymer concentration ($p < 0.0001$) and were greater for redox-

Table 2
Volumetric swelling ratio (Q), molecular weight between crosslinks ($\bar{M}_c$), mesh size (ζ), and crosslinking densities (ρ) of UV- and redox-cured hydrogels

Crosslinking method	[Polymer] (%)	Q	$\bar{M}_c$	ζ (Å)	ρ ($\times 10^{-4}$ mol/cm^3)
UV	10	10.8 (1.0)	1914	94	6.6
	15	7.0 (0.3)	1114	62	11.4
	20	5.5 (0.3)	762	48	16.6
Redox	10	11.8 (2.1)	2801	117	4.5
	15	8.0 (0.2)	1815	83	6.9
	20	6.6 (0.9)	1420	69	8.9

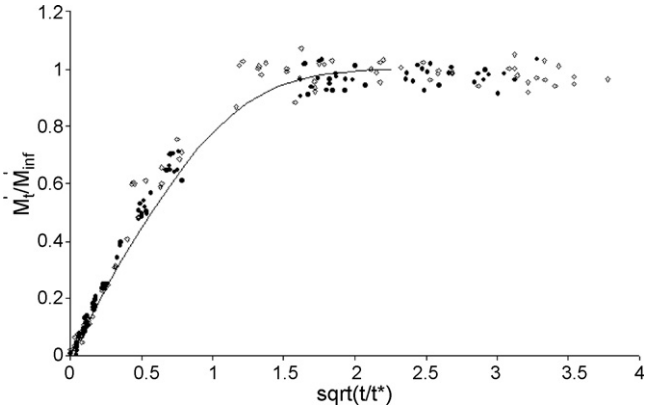

Fig. 2. Transformed amount released of FD20 from: (♦) redox and (◊) UV-cured 10% hydrogels. The solid line represents theoretical release from a cylinder.

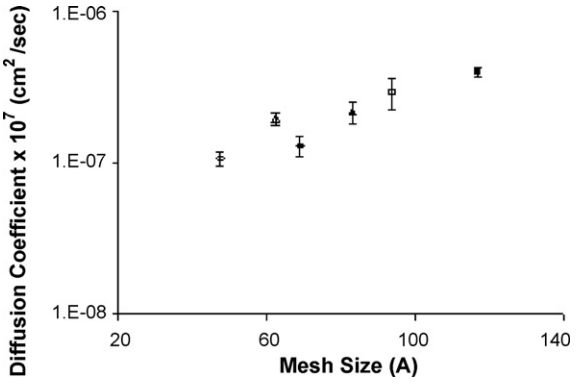

Fig. 3. Diffusion coefficient (D) plotted in logarithmic scale versus the mesh size of: (□) 10%, (△) 15%, and (◊) 20% UV-cured hydrogels, and (■) 10%, (▲) 15%, and (♦) 20% redox-cured hydrogels. Error bars represent standard deviations calculated from three runs.

cured hydrogels ($p = 0.004$). From the equilibrium swelling studies, increasing the solid content resulted in networks of higher crosslinking density and lower mesh sizes (see Table 2). Since diffusion of the solute occurs through the open spaces between the macromolecular chains, release rate of the drug is expected to be lowered as the mesh size is decreased. In addition, the higher diffusion coefficients achieved from redox-cured hydrogels can be explained by the higher mass loss observed from redox-cured networks that subsequently led to higher mesh sizes. Fig. 3 shows a plot of the diffusion coefficients versus the mesh sizes. As expected, experimental diffusion coefficient increased in direct proportion to the calculated mesh size. This is in agreement with trends reported in the literature (Hickey and Peppas, 1995; Peppas and Reinhart, 1983; Smith and Sefton, 1988; Reinhart and Peppas, 1984). However, while trends observed between diffusion coefficients and mesh sizes or solute MWs can be drawn within one study, no conclusion can be inferred when comparing different studies. This restriction might be due to network properties such as PVA backbone and curing techniques.

The experimental release data were compared to a theoretical model based on diffusion from an infinite cylinder. The theoretical diffusion coefficient was calculated according to Eq. (12). Fig. 4 shows experimental and theoretical D in relation to the polymer concentration. Experimental values of D were lower than the theoretical values. This may be due to temporary interactions between FD and the polymer, drug distribution and non-ideal nature of the network. The Davis model does not take drug–polymer interactions into consideration. FD contains hydroxyl groups and may form

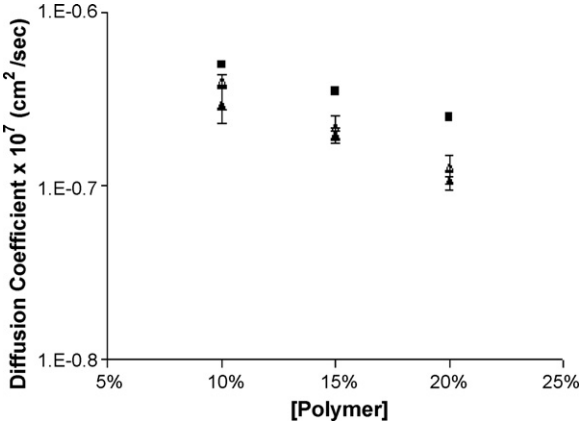

Fig. 4. Diffusion coefficients plotted in logarithmic scale as function of polymer concentration. Experimental D of (▲) redox, (△) UV-cured hydrogels and (■) theoretical D calculated according to Davis model shown in Eq. (12).

Table 3
% Total release, total release time and diffusion coefficients of FD20 from PVA hydrogels

Crosslinking method	[Polymer] (%)	%Burst release	% Total release	Characteristic time (h)	D ($\times 10^7$ cm^2/s)
UV	10	5.19 (1.73)	49.3 (18.5)	12.0 (2.8)	2.92 (0.38)
	15	7.83 (2.85)	40.4 (15.9)	15.5 (1.5)	1.95 (0.20)
	20	8.72 (2.28)	41.2 (11.2)	42.7 (7.7)	1.07 (0.30)
Redox	10	5.30 (2.33)	54.6 (9.0)	7.7 (0.7)	4.00 (0.45)
	15	4.60 (1.36)	61.9 (7.6)	13.6 (2.7)	2.17 (0.32)
	20	5.42 (0.82)	68.3 (11.2)	23.7 (3.1)	1.30 (0.19)

Mean (standard deviation), $n = 3$.

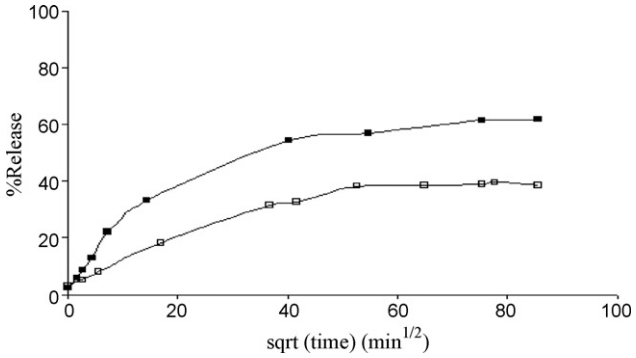

Fig. 5. % Release of FD20 from: (■) redox and (□) UV-cured 15 wt.% hydrogels. The solid line is to guide the eye.

temporary H-bonding with the pendant hydroxyl groups of PVA slowing down its diffusion rate. In addition, the model is based on uniform distribution of the drug in the cylinder. No assessment has been conducted to investigate if the loaded hydrogels are homogeneous.

As discussed previously network structure is based on average crosslink densities (and mesh sizes) with considerable variation expected due to polydispersity of the PVA backbone chains and the statistical nature of functionalisation of the chains. Similar deviation from theoretical diffusion coefficients has been reported in the literature, and has been related to different factors such as hydrodynamic friction (Leloup et al., 1990; Claeys and Arnold, 1989), solute-drug interaction and experimental artefacts such as boundary layer resistance (Gehrke et al., 1997; Liu et al., 2001). Furthermore, experimental diffusion coefficients of redox-cured hydrogels were closer to the theoretical values than their corresponding UV-cured hydrogels. This might be related to the lower crosslinking density associated with the redox networks, and thus less physical entrapment of the solutes is expected to occur in the more open structure of these networks. Also, redox-cured hydrogels appeared to uptake water which facilitates the diffusion of solutes, compared to UV-cured hydrogels that lost water and thus might have slowed down solute diffusion.

Fig. 5 is an illustrative example of the % release of FD20 from 15 wt.% UV- and redox-cured hydrogels. The total release of model drug (including the burst %) from the hydrogel system was in the order of 40–50% from UV hydrogels whereas release from redox-cured hydrogels was higher at between 55 and 70%.

Although the variability was higher between experiments, it is clear that a higher percentage is released from redox hydrogels over shorter time spans. To investigate whether the incomplete release of the drug was due to size exclusion or interaction between the drug and the polymer, a lower molecular weight drug, FD4 (FITC-Dextran, 4 kDa), of same chemical and physical properties as FD20 was loaded in 10 and 15 wt.% UV-cured hydrogels. The experimental release data were transformed as discussed in Section 2.

A higher percent release equivalent to 85% of FD4 loaded was achieved from the 10 and 15 wt.% UV-cured hydrogel as compared to 50 and 40% release of FD20 from the 10 and 15 wt.% UV-cured hydrogels, respectively. Also, both hydrogels showed a characteristic time of 7 h for release of FD4 while the characteristic time for release of FD20 was ~12 and 15 h from 10 and 15 wt.% hydrogels, respectively. The higher experimental diffusion coefficient of FD4 calculated from the slope (9.43×10^{-7} cm^2/s for 10%, and 8.07×10^{-7} cm^2/s for 15%) confirms its rapid release compared to FD20. This result is in agreement with other studies that investigated the effect of varying the MW of the solute on its release rate as with the work of Burczak et al. (1994) where diffusion coefficients decreased from $\sim 5 \times 10^{-7}$ to 6×10^{-8} cm^2/s as MWs of the solutes increased from ~6 to 67 kDa. Hence, achieving higher release of FD4 over a shorter period of time indicates that the higher MW drug is more likely to be physically entrapped inside the network rather than due to permanent interactions with the polymer. However, FD20 has a Stokes' radius (33 Å, as reported by the supplier) smaller than the average mesh size of all hydrogel variants. The physical exclusion observed is likely a result of the wide variation of actual mesh sizes. Calculated mesh sizes are an average value of the whole network comprising domains with different crosslinking densities. These so called microgel domains (Scotchford et al., 1998) can have mesh sizes small enough to entrap solute molecules and restrict their diffusion. The large variation in the total amount released, observed between experiments conducted on different days (more so with UV-cured hydrogels), precluded detecting differences between curing techniques ($p = 0.1486$). This variation might have occurred due to experimental errors such as variation in the cylinder dimensions and error in the estimation of the loaded amount of FITC-Dextran.

In a similar study by Bourke et al. (2003), release of platelet-derived growth factor (PDGF) was assessed from UV-cured hydrogels of comparable solid content. Release profiles and release amounts of the growth factors were similar to the results obtained in this study. In addition, the study showed that PDGF retained its biological activity following its encapsulation and release. This suggests that similar PVA networks can be potentially used as delivery systems for the release of biologically active proteins.

4. Conclusion

In this study, structural and diffusional properties of PVA hydrogels cured by UV and redox initiation were characterised as a potential biomaterial that can cure *in situ* and function as a drug delivery system for the controlled release of macromolecules.

The results showed changes of parameters influencing the crosslinking density of the polymer network such as the polymer concentration, and the crosslinking method lead to the generation of hydrogels of different structural properties and hence different release kinetics. The duration of drug delivery from PVA hydrogels can be varied from hours to ~2 days by increasing the solid content in the network.

The crosslinking methods followed proved to be efficient in preparing networks of controlled structural properties. However, redox curing has the advantage of *in situ* curing following injection of the aqueous macromer solutions with the drug dissolved within. Redox initiation is of particular interest since it has the advantage of *in situ* polymerization, and thus an appropriate technique for the implantation of a delivery system into the body.

References

Anseth, K.S., Wang, C.M., Bowman, C.N., 1994. Kinetic evidence of reaction diffusion during the polymerization of multi (meth) acrylate monomers. Macromolecules 27, 650–655.

Anseth, K.S., Metters, A.T., Bryant, S.J., Martens, P.J., Elisseeff, J.H., Bowman, C.N., 2002. In situ forming degradable networks and their application in tissue engineering and drug delivery. J. Control. Release 78, 199–209.

Armitage, P., Berry, G., 1994. Statistical Methods in Medical Research, 3rd ed. Blackwell, Melbourne.

Berkowitch, J., Charlesby, A., Desreux, V., 1957. Radiation effects on aqueous solutions of PVA. J. Polym. Sci. 25, 490–492.

Bo, J., 1992. Study on PVA hydrogels crosslinked by epichlorohydrin. J. Appl. Polym. Sci. 46, 783–786.

Bourke, S.L., Al khalili, M., Briggs, T., Michniak, B.B., Kohn, J., Poole-Warren, L.A., 2003. A photo-crosslinked poly(vinyl alcohol) hydrogel growth factor release vehicle for wound healing applications. AAPS Pharm. Sci. 5.

Bryant, S.J., Nuttelman, C.R., Asenth, K.S., 2000. Cytocompatibility of UV and visible light photo-initiating systems on cultured NIH/3T3 fibroblasts in vitro. J. Biomater. Sci. Polym. Ed. 11, 439–457.

Burczak, K., Fujisato, T., Hatada, M., Ikada, Y., 1994. Protein permeation through poly(vinyl alcohol) hydrogel membranes. Biomaterials 15, 231–238.
Claeys, I.L., Arnold, F.H., 1989. Nuclear magnetic relaxation study of hindered rotational diffusion in gels. AIChE J. 35, 335–338.
Crank, J., 1975. The Mathematics of Diffusion, 2nd ed. Oxford University Press Inc., New York.
Cruise, G.M., Scharp, D.S., Hubbell, J.A., 1998. Characterization of permeability and network structure of interfacially photopolymerized poly(ethylene glycol) diacrylate hydrogels. Biomaterials 19, 1287–1294.
Davis, B.K., 1974. Diffusion in polymer gel implants. Proc. Natl. Acad. Sci. U.S.A. 71, 3120–3123.
Einstein, A., 1956. Investigations on the Theory of the Brownian Movement. Dover Publications, Inc.
Gehrke, S.H., Fisher, J.P., Palasis, M., Lund, M.E., 1997. Factors determining hydrogel permeability. Ann. N.Y. Acad. Sci. 831, 179–184.
Hassan, C.M., Stewart, J.E., Peppas, N.A., 2000. Diffusional characteristics of freeze/thawed poly(vinyl alcohol) hydrogels: applications to protein controlled release from multilaminate devices. Eur. J. Pharm. Biopharm. 49, 161–165.
Hickey, A.S., Peppas, N.A., 1995. Mesh size and diffusive characteristics of semicrystalline poly(vinyl alcohol) membranes prepared by freezing/thawing techniques. J. Membr. Sci. 107, 229–237.
Langer, R., 1998. Drug delivery and targeting. Nature 392, 5–10.
Leloup, V.M., Colonna, P., Ring, S.G., 1990. Studies on probe diffusion and accessibility in amylose gels. Macromolecules 23, 862–866.
Li, J., Ni, X.W., Leong, K.W., 2003. Injectable drug-delivery systems based on supramolecular hydrogels formed by poly(ethylene oxide)s and α-cyclodextrin. J. Biomed. Mater. Res. 65A, 196–202.
Liu, Z., Cheung, R., Wu, X.Y., Ballinger, J.R., 2001. A study of doxorubicin loading onto and release from sulfopropyl dextran ion-exchange microspheres. J. Control. Release 77, 213–224.
Martens, P., Grant, M., Nilasaroya, A., Whitelock, J., Poole-Warren, L.A., 2008. Characterisation of redox initiators for producing poly(vinyl alcohol) hydrogels. Macromol. Symp. 266, 59–62.
Mawad, D., Martens, P., Odell, R.A., Poole-Warren, L.A., 2007. The effect of redox polymerisation on degradation and cell responses to poly(vinyl alcohol) hydrogels. Biomaterials 28, 947–955.
Mellot, M.B., Searcy, K., Pishko, M.V., 2001. Release of protein from highly crosslinked hydrogels of poly(ethylene glycol) diacrylate fabricated by UV polymerization. Biomaterials 22, 929–941.
Mongia, N.K., Anseth, K.S., Peppas, N.A., 1996. Mucoadhesive poly(vinyl alcohol) hydrogels produced by freezing/thawing processes: applications in the development of wound healing systems. J. Biomater. Sci. Polym. Ed. 7, 1055–1064.
Nguyen, K.T., West, J.L., 2002. Photopolymerizable hydrogels for tissue engineering applications. Biomaterials 23, 4307–4314.
Patel, A.A., Solomon, J.A., Soulen, M.C., 2005. Pharmaceuticals for intra-arterial therapy. Semin. Int. Radiol. 22, 130–138.
Peppas, N.A., Merrill, E.W., 1977. Crosslinked poly(vinyl alcohol) hydrogels as swollen elastic networks. J. Appl. Polym. Sci. 21, 1763–1770.
Peppas, N.A., Reinhart, C.T., 1983. Solute diffusion in swollen membranes. Part I. A new theory. J. Membr. Sci. 15, 275–287.
Peppas, N.A., 1987. Hydrogels in Medicine and Pharmacy: Fundamentals, vol. I. CRC Press Inc., Boca Raton, FL, pp. 57–83.
Peppas, N.A., Bures, P., Leobandung, W., Ichikawa, H., 2000. Hydrogels in pharmaceutical formulations. Eur. J. Pharm. Biopharm. 50, 27–46.
Reinhart, C.T., Peppas, N.A., 1984. Solute diffusion in swollen membranes. Part II. Influence of crosslinking on diffusive properties. J. Membr. Sci. 18, 227–239.
Sarac, A.S., 1999. Redox polymerization. Progr. Polym. Sci. 24, 1149–1204.
Scotchford, C.A., Cascone, M.G., Downes, S., Giusti, P., 1998. Osteoblast responses to collagen-PVA bioartificial polymers in vitro: the effects of crosslinking method and collagen content. Biomaterials 19, 1–11.
Shu, X.Z., Liu, Y., Palumbo, F.S., Luo, Y., Prestwich, G.D., 2004. In situ crosslinkable hyaluronan hydrogels for tissue engineering. Biomaterials 25, 1339–1348.
Siskin, G.P., Englander, M., Stainken, B.F., Ahn, J., Dowling, K., Dolen, E.G., 2000. Embolic agents used for uterine fibroid embolization. AJR Am. J. Roentgenol. 175, 767–773.
Smith, B.A., Sefton, M.V., 1988. Permeability of a heparin-poly(vinyl alcohol) hydrogel to thrombin and antithrombin III. J. Biomed. Mater. Res. 22, 673–685.
StataCorp, 1999. Stata Statistical Software: Release 6.0. Stata Corporation, College Station, TX.
Yamaoka, T., Tabata, Y., Ikada, Y., 1995. Fate of water-soluble polymers administered via different routes. J. Pharm. Sci. 84, 349–354.